Energetic particle propagation in the inner heliosphere as deduced from low-frequency (<100 kHz) observations of type III radio bursts

H. V. Cane[1]
NASA Goddard Space Flight Center, Greenbelt, Maryland, USA

W. C. Erickson
Bruny Island Radio Spectrometer, Bruny Island, Tasmania, Australia

Received 15 May 2002; revised 20 January 2003; accepted 25 February 2003; published 21 May 2003.

[1] Solar energetic particle (SEP) events are well-associated with solar flares. It is observed that the delay between the time of the flare and the first-arriving particles at a spacecraft increases with increasing difference between the flare longitude and the foot point of the field line on which the spacecraft is located. This difference we call the "connection angle" and can be as large as ~120°. Recently it has been found that all SEP events are preceded by type III radio bursts. These bursts are plasma emission caused by the propagation of 2–50 keV flare electrons through the solar corona and into the solar wind. The drift of these type III radio bursts to lower and lower frequencies enables the propagation of the flare electrons to be traced from the Sun to about 1 AU. We have made an extensive analysis of the type III bursts associated with >20 MeV proton events and find that, in most cases, the radio emission extends to the local plasma frequency when the energetic particles arrive within a few hours of the flare. We conclude that this emission at the lowest possible frequency is generated close to the spacecraft. We then use the time from when the burst started at the Sun to when it reached the local plasma frequency to infer the time it took the radio producing electrons to travel to the spacecraft. We find that these delay times are organized by the connection angle and correlate with the proton delay times. We also find that the differences between the radio delays at Wind and Ulysses are matched by differences in the relative arrival times of the energetic particles at the two spacecraft. The consistent timing between the relative arrival times of energetic electrons and protons and the start of the lowest frequency radio emissions suggests that the first arriving particles of both species are accelerated as part of the flare process and that they propagate to the spacecraft along trajectories similar to those of the lower-energy flare electrons. To be detected by observers at locations distant from the nominal field lines originating in the flaring regions the particles must undergo lateral transport. The continuity of the radio bursts suggests that the cross-field transport occurs in the interplanetary medium. *INDEX TERMS:* 7514 Solar Physics, Astrophysics, and Astronomy: Energetic particles (2114); 7534 Solar Physics, Astrophysics, and Astronomy: Radio emissions; 7859 Space Plasma Physics: Transport processes; 7519 Solar Physics, Astrophysics, and Astronomy: Flares; *KEYWORDS:* Energetic particles, radio emissions, flares, energetic particle transport

Citation: Cane, H. V., and W. C. Erickson, Energetic particle propagation in the inner heliosphere as deduced from low-frequency (<100 kHz) observations of type III radio bursts, *J. Geophys. Res.*, *108*(A5), 1203, doi:10.1029/2002JA009488, 2003.

1. Introduction

[2] Recently it has been determined that solar proton events are well-associated with type III bursts [*Cane et al.*, 2002]. A list of events seen near Earth in the period 1997–mid-2001, and the relevant parameters, was presented. In this paper in situ measurements of energetic protons and electrons are compared with the low frequency extents and drift rates of their associated type III radio bursts. We find a correlation between the arrival times of 38–53 keV electrons, >10 MeV protons and the times at which the associated type III burst reaches the local plasma frequency at the observer. This correlation is maintained for spacecraft near Earth, (WIND, ACE and IMP 8) and at Ulysses even though the arrival times of the particles and radio waves may differ by several hours between the two spacecraft when they are distant from each other.

[3] Type III bursts are produced when beams of electrons in the 2–~50 keV range generate emission at the local

[1]Also at Bruny Island Radio Spectrometer, Bruny Island, Tasmania, Australia.

0148-0227/03/2002JA009488$09.00

plasma frequency [see, e.g., *Bastian et al.*, 1998]. Although emission at the first harmonic of the plasma frequency may also be generated, *Dulk* [2000] gives various arguments indicating that at the low frequencies of interest to the present study the initial radiation is almost always fundamental emission. Type III radio bursts drift to lower and lower frequencies when the electron beam successively encounters lower and lower plasma densities in the corona and interplanetary medium. When the electron beam reaches the vicinity of an observer the emission reaches the local plasma frequency and no lower frequency emission is observed. Radio waves cannot propagate below the local plasma frequency.

[4] Type III bursts are well associated with flares, indeed the responsible electrons are a basic element of the flare process. When type III bursts continue below 10 MHz (corresponding to a distance of 2–3 solar radii above the solar surface) then it is clear that there are open field lines from the flaring region. Escaping electrons are detected in situ if they gain access to field lines that intercept the observer. Short duration electron increases detected in space are essentially always accompanied by type III radio bursts at low frequencies (below ~1 MHz) [*Lin*, 1985]. Many bursts are observed below ~1 MHz but we argue that only if the burst reaches a 1AU observer's local plasma frequency will energetic electrons also be detected i.e. we suggest that any emission near the observer's local plasma frequency is locally generated. *Dulk et al.* [1998] find a relationship between the intensity of emission and the number density of electrons. Thus some weaker electron streams do not produce bursts extending to the plasma frequency at 1 AU and there also appears to be an intrinsic cutoff of type III emission at about 10 kHz [*Leblanc et al.*, 1995].

[5] In section 2.1 we illustrate the basic result i.e. that there is a fixed relationship between the arrival of ~40 keV electrons, of >10 MeV protons and the extension of the associated type III burst to the local plasma frequency. Section 2.2 presents the results of a statistical analysis for 127 proton events detected near Earth. In Section 2.3 we compare similar data sets but for two locations in the inner heliosphere. In Section 3 we discuss the results. We conclude that in most events the first arriving particles are accelerated by the flare process. In many cases there is unlikely to be direct magnetic connection via a Parker field to the source region and so there must be some lateral transport either at the Sun or in the interplanetary medium. Since the radio burst is continuous in every event between the high frequencies that are generated near the flaring region and the observer's plasma frequency this suggests cross field transport in the interplanetary medium. In any case it is clear that understanding these data is vital to understanding longitudinal particle transport.

2. Data Analysis

[6] This study uses radio and particle data from the Wind, ACE, Ulysses and IMP 8 spacecraft. The radio data are from the WAVES experiment (PI's M. L. Kaiser and J.-L. Bougeret) on the Wind spacecraft [*Bougeret et al.*, 1995] and the URAP experiment (PI R. J. MacDowall) on Ulysses [*Stone et al.*, 1992]. The WAVES radio data cover the frequency range 13.825 MHz to 4 kHz and the Ulysses radio data cover the frequency range 940 kHz to 1 kHz. The WAVES data were obtained from the NSSDC CDAW Internet site and the URAP data from the URAP home page. Electron data were obtained from identical experiments (HI-SCALE and EPAM) on Ulysses and ACE respectively. Data from the HI-SCALE experiment [*Lanzerotti et al.*, 1992] were obtained from the Ulysses site maintained at ESA whereas data from the EPAM experiment (PI R. E. Gold) were obtained from NSSDC. The experiments cover the energy range 34–315 keV in 4 channels. The Ulysses proton data were obtained from the HET component of the COSPIN experiment [*Simpson et al.*, 1992] (PI R. B. McKibben) via the ESA Ulysses website. Finally, the IMP 8 proton data were obtained from the GSFC experiment [*McGuire et al.*, 1986].

2.1. Sample Events at 1 AU

[7] To illustrate the procedure that was employed in this paper, Figure 1 shows radio dynamic spectra and particle intensity profiles for four events with different timing characteristics. Only data from the TNR receiver of the WAVES experiment are shown in order to illustrate in more detail the behaviour at the lowest frequencies. Each of the left-hand panels of radio data shows 5 hours of data covering the frequency range 245 to 10 kHz. The grey shading represents the intensities at each frequency as a function of time (3 minute averages); the grey scale has been adjusted to enhance the low-frequency features. The left hand edge of each plot starts 30 minutes before the onset of the burst at 14 MHz. The start time of the burst at 14 MHz is given at the top of each panel. A vertical line is shown at this time and at 60 minute intervals thereafter. The thin grey intensi-

Figure 1. (opposite) (Left) Dynamic spectra in the range 245 kHz to 10 kHz for four 5 hour periods from the WAVES experiment on Wind. The vertical lines are every 60 minutes, the first one is at the time the burst group starts at 14 MHz. For the event in the upper panel the delay between when the burst starts and when it reaches the plasma line near 20 kHz (indicated by small arrow outside right edge of panel) is approximately 30 minutes. The dashed line to the left of the burst indicates the low frequency drift rate. For the event in the next panel the delay is about 1.5 hours. The delay is uncertain for the event in the third panel. Although the burst looks similar to the one above, it is important to note that the plasma frequencies are different. Thus the lower event must take longer to get to the plasma frequency. In fact it fades out at a higher frequency. For the bottom event the leading edge of the burst becomes parallel to the plasma line and does not intercept it. These events had connection angles of 23°, 9°, 57° and −86°. (The vertical dark areas, with horizontal cutoffs, at the leading edges of the bursts are instrumental and caused by saturation of the digital receiver.) (Right) 38–53 keV electron and 11–23 MeV proton intensities at ACE and IMP 8, respectively. The intensity scale is for the electrons only. The proton intensities are arbitrary. They are of the order of 10^{-5} lower than the electron intensities. Note that as the radio delays get longer the particles increase more gradually and later.

fication that wiggles its way approximately horizontally across each dynamic spectrum near 20 kHz (in these examples) (and indicated by an arrow outside the right hand edge of the panel) is called the "plasma line". It results from thermal noise in the plasma surrounding the antenna [*Meyer-Vernet and Peche*, 1989] and allows immediate determination of the local plasma frequency. The arrow at the bottom of each panel indicates the approximate interval between the start time of the burst at 14 MHz and the intersection of the leading edge of the burst, or its extrapolation, with the plasma line. Short dashed lines indicate the slopes of the leading edges of the bursts. Although the interval (which we call the radio delay) is difficult to determine accurately, it increases from about 30 minutes for the first event to about two hours in the third event. The fourth event shows an example where the type III burst (or even its extrapolation) clearly did not reach the plasma line.

[8] The right-hand panels show electron data (38–53 keV) and proton data (11–23 MeV). For clarity the proton intensity scale is not shown; the proton intensities in this energy range are about a factor of 10^{-4}–10^{-5} below the

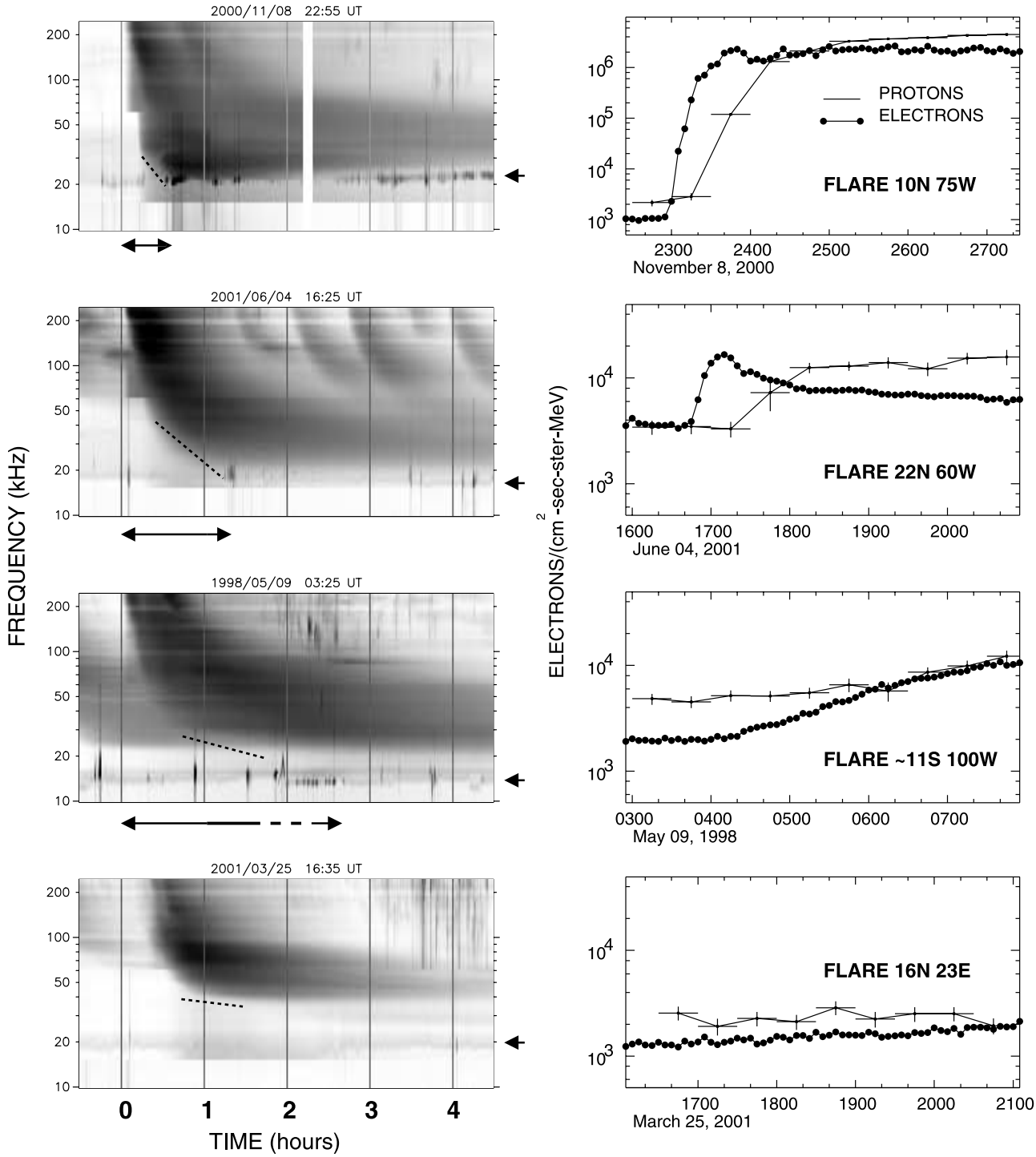

electron intensities. The top event of November 8, 2000 was associated with an M7 flare at 10°N 75°W. The solar wind speed of 440 km/s implies that, under the assumption of a simple spiral interplanetary magnetic field, the spacecraft was on a field line connected to longitude 52°W. The difference from the flare longitude, which we call the connection angle, was therefore 23°. The other events were associated with flares at 22°N 60°W, ~11°N 100°W and 16°N 23°E and had connection angles of 9°, 57° and −86°. The top two events, with connection angles of <30° were magnetically well connected to Earth and the particle intensities rose rapidly. The radio burst delays between the start time near the Sun and the leading edge close to the plasma line were less than 1.5 hours. The November 8, 2000 particle event was very intense and a different intensity scale is used for this event. Note that the radio burst is intense at the lowest frequencies (black in the figure) and this is probably because the particle event is so intense. The dark intensifications of the plasma line near the first hour mark are caused by Langmuir waves. The event of May 9, 1998 occurred behind the west limb of the Sun and is presumed to be from the same region that produced several large events when it was on the disk. The particle intensities for this event and the one on March 25, 2001 rose slowly and the radio bursts either did not extend clearly to the plasma line (for the 1998 event) or cut off well above the plasma line (for the 2001 event). Note that in all cases the ordering is such that the 38–53 keV electrons arrive first, followed by the 11–23 MeV protons and finally by the leading edge of the burst extending to the plasma line. The ordering suggests that the radio producing electrons and the first arriving higher energy electrons and protons could have a common origin. In the next section we summarize the results of a similar analysis on many events.

2.2. Statistical Study of Many Events at 1 AU

[9] We have examined the type III bursts associated with some ~130 proton events detected above 20 MeV with the GSFC IMP 8 experiment in the period 1997–2001, based on the *Cane et al.* [2002] list with the addition of events that occurred in 2001, after the end of this list. Figure 2 presents results for all 127 events in which the radio delay (as indicated in Figure 1) can be determined. (If the radio burst definitely did not extend to the plasma line, as in the bottom panel of Figure 1, a delay of 7 hours is adopted.) The radio delays are plotted vs. connection angle. The connection angle orders the radio delays rather well, despite the fact that the connection angle may be inaccurate for some events. For example the magnetic field will deviate from a simple spiral when the Earth is inside the looped field of an interplanetary coronal mass ejection. Also the connection angles greater than +30° correspond to events behind the west limb and are therefore only approximate. The extent to which an event is well connected will also vary if the source region itself varies in size, as it would if, for example, it is related to the size of the associated flaring region The events that do not extend to the plasma line all have connection angles outside the range ±25°, i.e., all well-connected events have radio bursts that extend to the plasma line. Apart from one event, the delays are shortest for events within −40 to +60 degrees, and there is a tendency for the delays to become longer with increasing connection angle. The

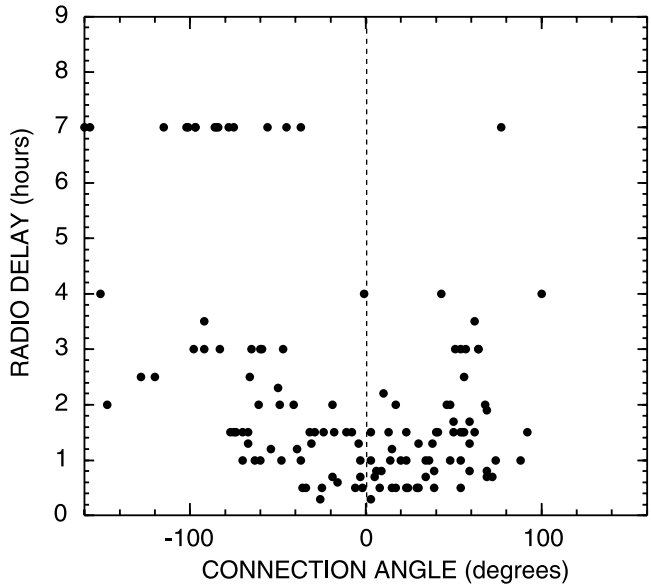

Figure 2. Radio burst delays, as illustrated in the previous figure, are shown as a function of the magnetic connection of IMP 8 to the associated flare for >20 MeV proton events. Delays of 7 hours correspond to events in which the burst did not intersect the plasma line. In some cases this may be caused by an intrinsic cutoff in the emission rather than a very low drift rate.

exceptional event with a radio delay of 4 hours and connection longitude of only −1° occurred on February 11, 2001. In this case the particles started gradually and had intensity profiles typical of an event from behind the west limb. Thus we suspect that the flare association is in error.

[10] The characteristics of the particle events associated with the radio bursts of Figure 2 are organized as illustrated in Figure 1. Intense rapidly rising particle increases are associated with bursts with short radio delays, slowly rising events with initial low intensities are associated with bursts that do not extend to the plasma line and other events are intermediate in both radio and particle drift rates/risetimes. In summary, the delays of the radio bursts appear to be organized by the location of the flare suggesting that our initial assumption that the extension of a radio burst to the plasma line only occurs when the electron beam intercepts an observer is correct. That the radio delays then organize particle intensities and risetimes, as shown in Figure 1, is not surprising given that these parameters are also known to be organized by the longitude of the associated flare [e.g., *Cane et al.*, 1988]. In the next section we illustrate this further by considering several events in which particle and radio data for a single event can be examined from two locations.

2.3. Ulysses and Near-Earth Comparison

[11] Next we compare radio and particle data from the Wind, ACE, IMP 8 and Ulysses spacecraft for eight 18-hour periods of interest in 2000–2001. For the Wind dynamic spectra there are 51 frequencies between 10^4 and 10 kHz and the data are 3 minute averages. For Ulysses there are 26 frequencies and the data are 2.4 minute averages. Noise in the Wind data at ~100–300 kHz is Auroral Kilometric Radiation (AKR). Figures 3–6 show contrasting examples

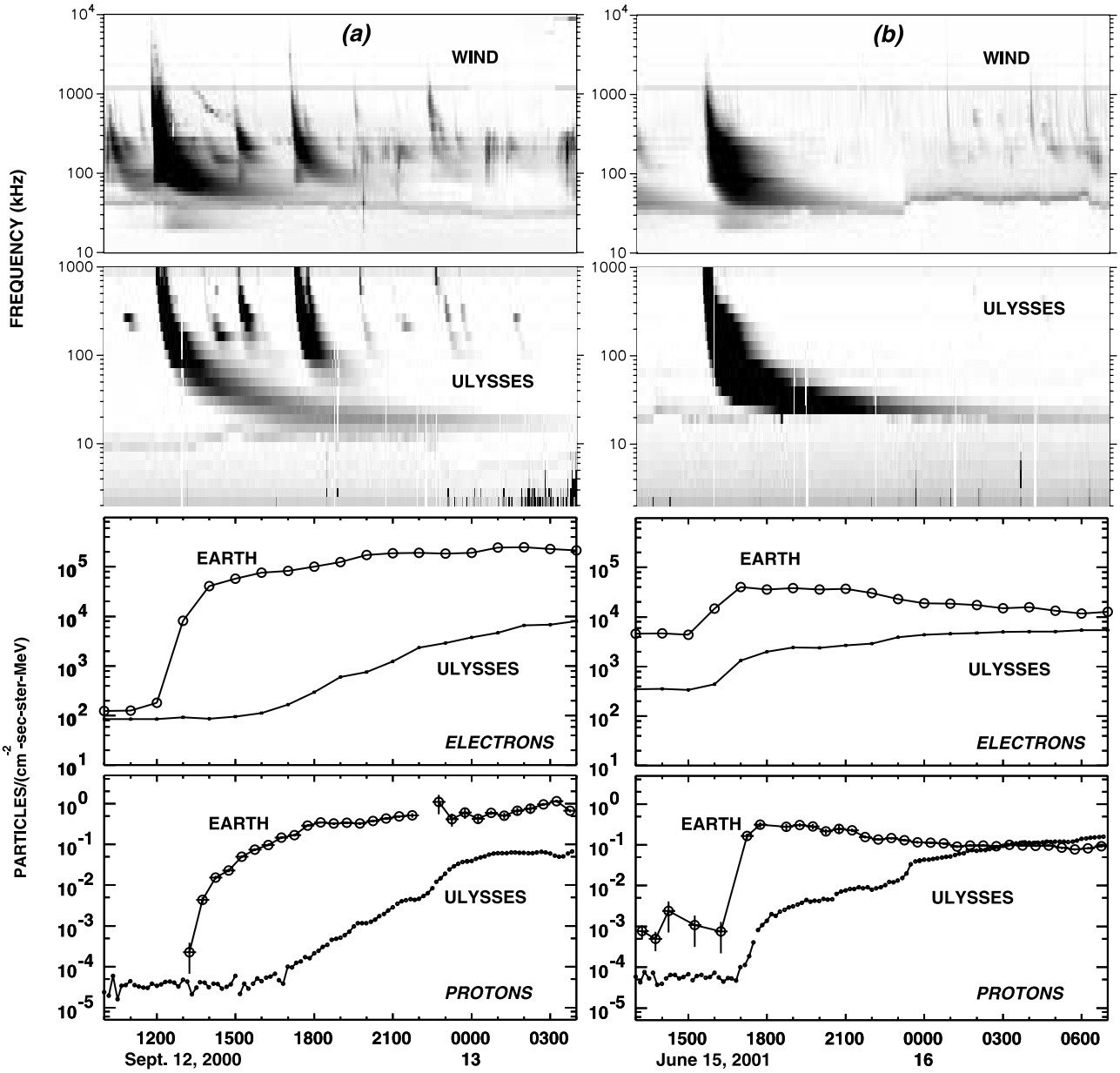

Figure 3. Radio and particle data from the Ulysses spacecraft and spacecraft near Earth. In Figure 3a both Ulysses and Wind saw an intense radio burst that drifted rapidly to the local plasma frequency at each spacecraft. The bottom panels compare electron and proton intensities. The electron data at Earth are from ACE (larger symbols) in the range 38–53 keV and at Ulysses from an identical experiment. Proton observations at Earth are from IMP 8 in the energy range 24–29 MeV. At Ulysses the proton intensities are in the range 14–19 MeV. The slow-drift feature at about 1400 UT and 1000 kHz seen by both spacecraft is radio emission from the CME-driven shock. The data in Figure 3b are quite similar to those in Figure 3a. On June 15, 2001 Ulysses was at only 1.4 AU and close to the ecliptic. The particle intensities rise earlier at Ulysses in the event of Figure 3b relative to those of the event of Figure 3a because of its closer proximity to the Sun; the magnetic connection was quite similar. Note that the radio burst extends to the plasma line more rapidly at Ulysses in Figure 3b compared with in Figure 3a consistent with the emission being generated locally when electrons approach the spacecraft.

in which both spacecraft had good magnetic connection to a solar event, or when one spacecraft had poor/no magnetic connection. Table 1 lists the events, the connection angles for both spacecraft and the location of Ulysses. The connection angle for Ulysses only takes into account its longitude. The events demonstrate that the drift rates of the type III bursts at low frequencies depend on the location of the spacecraft. Furthermore, if the bursts extend to the local plasma frequency, then energetic particles (electrons and protons) are observed.

[12] Figure 3a shows data for a period on September 12–13, 2000 when there were at least 10 type III bursts seen by

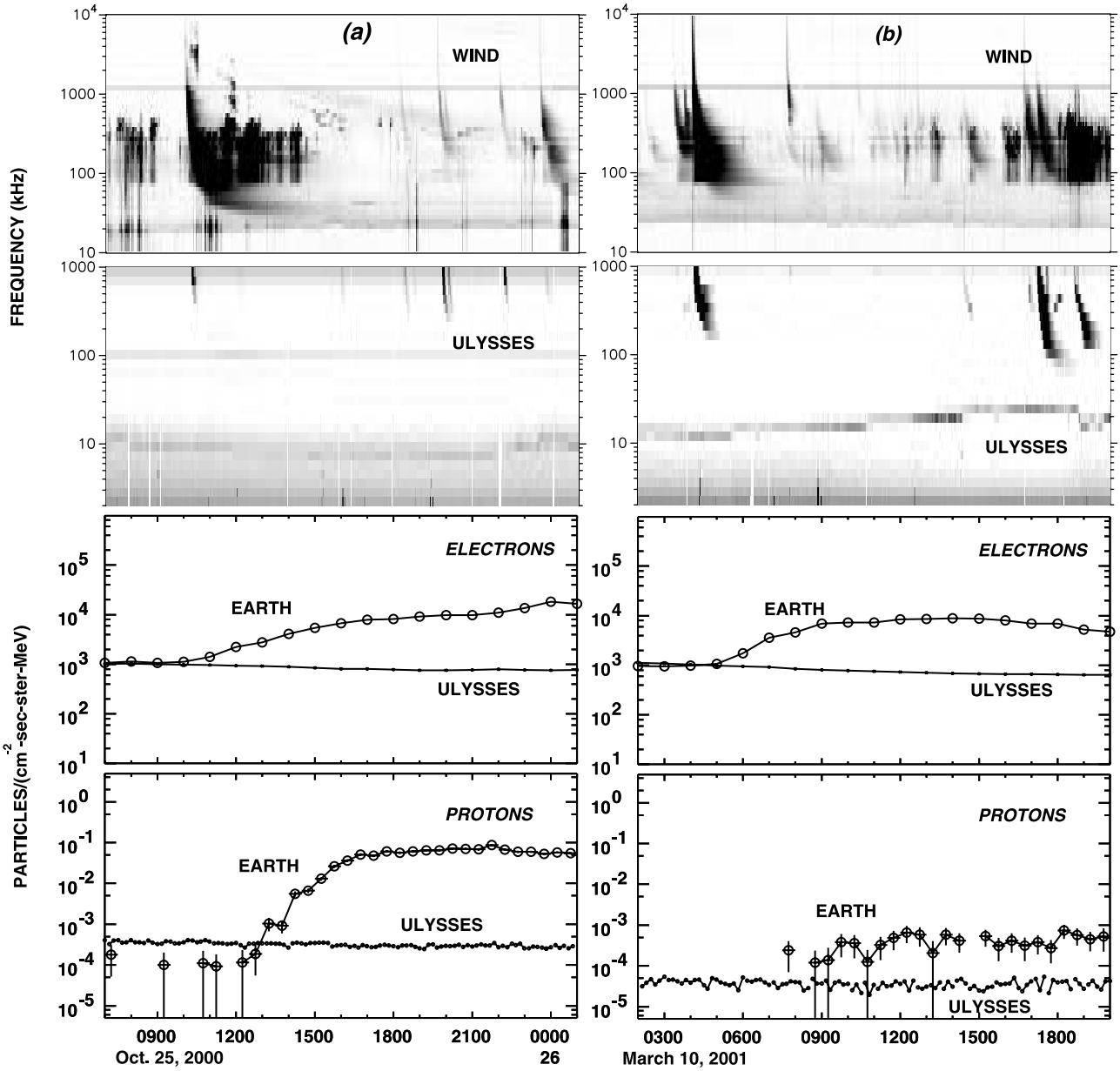

Figure 4. Same format as Figure 3. In these events there were prompt electron and proton events at Earth but not Ulysses, as seen in the lower panels. Magnetic connection was much better for Earth in both these cases. The radio bursts seen from Ulysses were weak and disappeared below 100 kHz. For both periods there was Auroral Kilometric Radiation seen at Wind in the approximate frequency range 100–400 kHz. In Figure 4b the absence of points for protons before 0745 UT is because IMP 8 did not detect any protons in the energy bin illustrated.

both spacecraft in the frequency range 100–1000 kHz. The most prominent burst occurred at ~1200 UT. Unlike most of the other bursts, it extended to the local plasma frequency at both spacecraft. (For this period the local plasma frequency ranged from 30 to 55 kHz near Earth and about 9 to 14 kHz at Ulysses.) This burst was associated with an M1 GOES soft Xray flare from 17°S 09°W at 1131 UT. Considering only the longitude of Ulysses it had a connection angle of about 11° compared to about +50° for Wind/IMP 8. However, Ulysses was almost 3 times further from the Sun. The bottom panels of Figure 3a show electron and proton data (~40 keV and ~25 MeV respectively) from Ulysses and near Earth. Note that the particles at each location begin to arrive just before the radio burst reaches the respective plasma line. As might be expected, given their different radial distances, the particles are seen first near Earth. However, it is surprising that the event was seen at all at Ulysses given its latitude was 71°S. Note that at both Ulysses and Earth the ~40 keV electrons arrive first, followed by the ~25 MeV protons, followed by the type III burst reaching the plasma line. This is consistent with the relative speeds of 0.4c, 0.2c and 0.17c (assuming 8 keV for the radio-producing electrons) and suggests that the first particles were accelerated at the same time and traveled

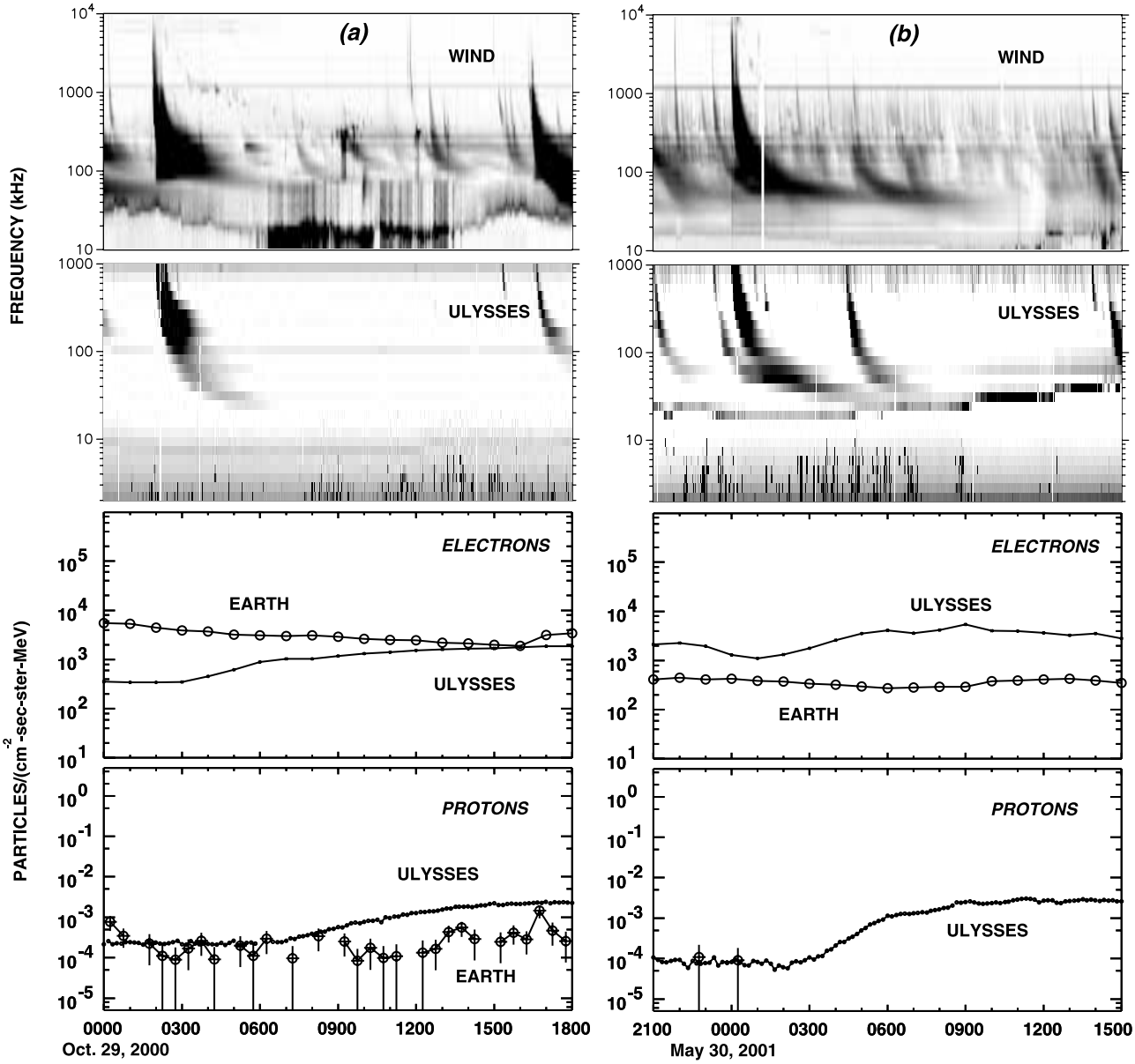

Figure 5. Same format as Figure 3. In both events the connection was better to Ulysses than to Earth and the particle event started first at Ulysses. (For the May 2001 event of Figure 5b particles were not seen near Earth until after the period illustrated.) For both events the leading edge of the burst at Wind became parallel to the plasma line at low frequencies. At Ulysses the burst of Figure 5a faded out below 20 kHz, probably because of an intrinsic cutoff of the emission.

similar paths. Detailed timing for this event indicates that the particles did not reach either spacecraft by traveling along simple Archimedian spirals [*Simnett*, 2001]. (Note that we illustrated a lower proton energy in Figure 1 because the IMP 8 experiment saturated above 25 MeV for the November 8, 2000 event.)

[13] Figure 3b shows another period (June 15–16, 2001) in which the connection to the solar event was quite similar for the two spacecraft. At this time Ulysses was at 24°N off the west limb of the Sun at 1.4 AU. No flare was observed at Earth because the event occurred behind the west limb of the Sun, probably at about W120°. (If the event had been closer to the west limb a soft Xray flare would have been seen [*Cane et al.*, 2002].) The event location is the reason why the radio event at Wind was weak above about 5 MHz i.e. the high-frequency emission was partially occulted. Otherwise, the radio bursts are similar in appearance at the two spacecraft, in part because they extend down to similar local plasma frequencies (~35 kHz at Wind and 25 kHz at Ulysses). The particle intensity-time profiles are fairly similar in the first 6 hours or so, apart from the reduced particle intensity at Ulysses since it was more distant from the Sun. Note that at each spacecraft, the onset of the particle event has the same timing relative to the radio burst reaching the plasma line as in Figure 3a. In conclusion, during the events in Figure 3, both radio bursts extended to the local plasma frequency and in situ electrons and protons were observed by Ulysses and near the Earth.

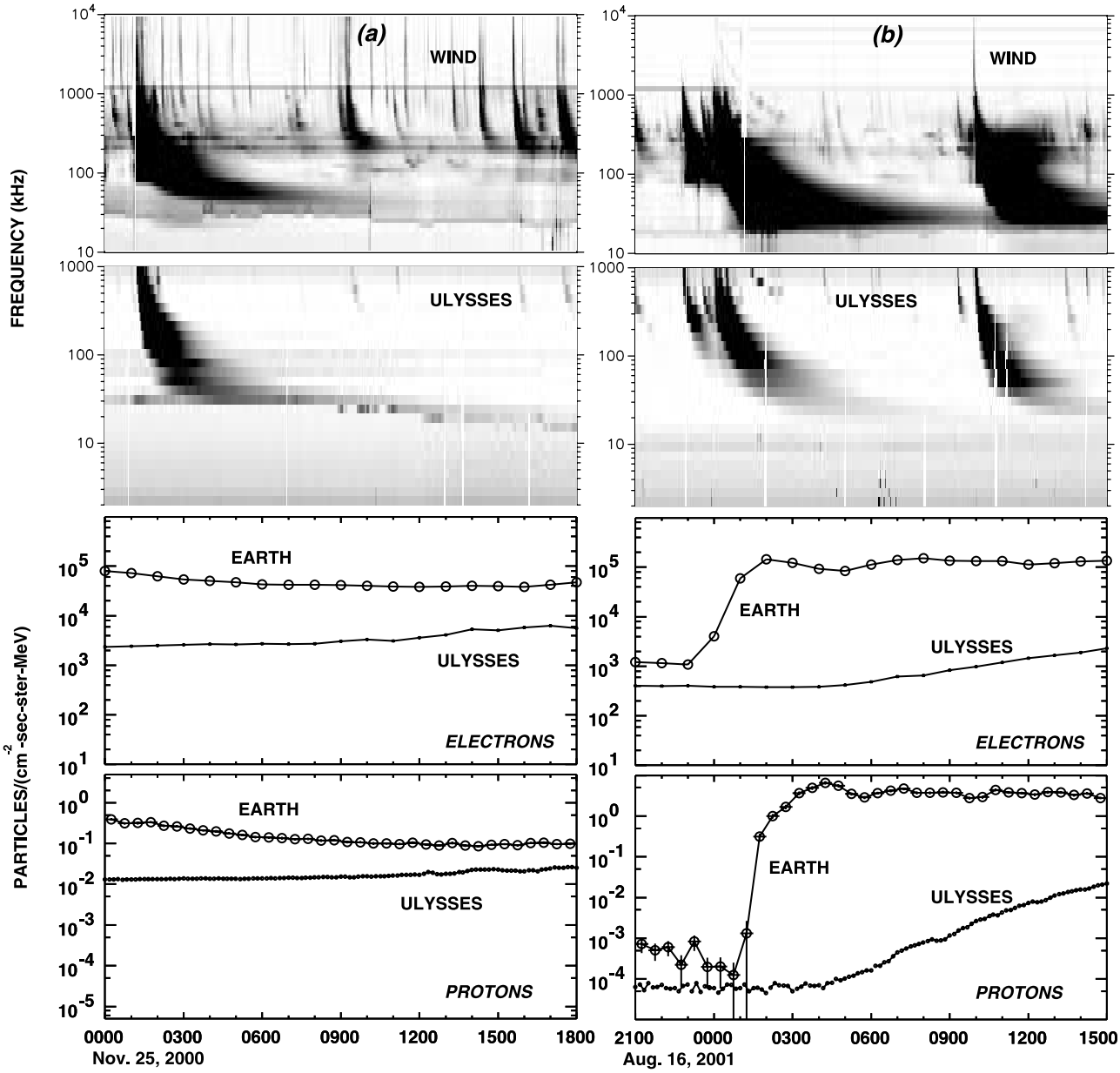

Figure 6. Same format as Figure 3. In these events the radio bursts extend to, or close to, the plasma lines at both spacecraft. The burst did so more rapidly at Ulysses for the event of Figure 6a and at Wind in the event of Figure 6b. In Figure 6a there was a high background from solar events on the previous day so new particle increases are difficult to discern. In Figure 6b the particle event started earlier at Earth.

[14] Figure 4 illustrates two events in which radio and in situ particle observations were quite different at Earth and Ulysses, in contrast to those in Figure 3. The event of interest in Figure 4a, at ~1000 UT on October 25, 2000, originated behind the west limb of the Sun. Because of the event location, the radio burst was weak above 1 MHz in the Wind data. It extended close to the plasma line at about 1500 UT. At Ulysses the radio event was insignificant and did not extend much below 400 kHz. Given that Ulysses was poorly connected, ~175° in longitude from the solar event, this is not surprising. The spiral field would bend away from the direction of Ulysses. As may be seen in the bottom panels there was no particle increase at Ulysses but one was observed at ACE and IMP 8. However, the particle intensities rose slowly, over a period of about 6 hours, compared with an hour or two for the events in Figure 3. The type III burst in the Wind data in Figure 4a also took longer to drift to the plasma line than the type III bursts in Figure 3. Note that, as in the event of Figure 3a, at the time of the October 25, 2000 event Ulysses was at a very southerly latitude of −78°. Both the Figure 3a and Figure 4a solar events originated in the southern hemisphere. Thus the lack of a radio burst at Ulysses in the event of Figure 4a is unlikely to be related to Ulysses' location in latitude.

[15] The event of interest in Figure 4b occurred at ~0400 UT on March 10, 2001. A type III burst was seen at both spacecraft but did not extend below 100 kHz at Ulysses. At Wind the burst is not very impressive and is partly masked

Table 1. SEP Events of Figures 3–6; Parameters at Earth and Ulysses

						Earth			Ulysses					
Figure	Date	DOY	Year	Time	Flare Location[a]	Footpt.[b]	Connect.[c] (deg.)	P[d]	Long. (deg.)	Footpt.[e] (deg.)	Connect. (deg.)	P	Lat.	Distance (AU)
3a	Sept. 12	(256)	2000	1145	17S 09W	59	−50	Y	197	358	11	Y	71S	2.8
3b	June 15	(166)	2001	1520	∼S 120W	72	48	Y	77	142	−22	Y	24N	1.4
4a	Oct. 25	(299)	2000	0955	∼S 120W	56	64	Y	176	305	175	...	78S	2.5
4b	March 10	(69)	2001	0400	27N 42W	53	−11	Y	157	231	171	...	47S	1.6
5a	Oct. 29	(303)	2000	0150	25S 35E	62	−97	...	176	341	−16	Y	78S	2.5
5b	May 29	(149)	2001	2355	∼S E95	62	−157	...	91	173	92	Y	10N	1.3
6a	Nov. 25	(330)	2000	0100	07N 50E	52	−102	...	185	336	−26	Y	80S	2.3
6b	Aug. 15	(227)	2001	2355	∼S 130W	47	83	Y	34	85	45	Y	63N	1.6

[a]Location of Hα flare or approximate location of likely active region.
[b]Solar longitude of foot point of field line near Earth.
[c]Difference between foot point and flare longitude. Value is negative if flare is to the east.
[d]Particles seen within a few hours of the solar event, Y, yes; ellipsis, no.
[e]This location only considers the longitude of Ulysses.

by AKR in the 100 kHz to 400 kHz range. The burst can be seen near 50 kHz but fades away before reaching the plasma line at about 25 kHz. The fading is likely a result of the fact that the number density of electrons became too low; a 40 keV electron event was seen at ACE along with a very weak 25 MeV proton event at IMP 8. No particle event was seen at Ulysses. The associated flare occurred at 24°N 42°W and was short in duration (<20 mins.). Earth was thus well connected whereas for Ulysses (about 70° beyond the west limb at 1.6 AU) the connection was 171°. Once again relative timings and lack of energetic particles at Ulysses suggest that the first arriving energetic particles and the type III-producing electrons are related.

[16] During both periods shown in Figure 5, a particle event was seen at Ulysses. While in one case, the event was very delayed at Earth in the other, it was not detected. The event of interest on October 29, 2000 (Figure 5a) was associated with a flare at 25°S 35°E at 0128 UT. At the time, Ulysses was at high southern latitudes, 176° west of Earth and at 2.5 AU. It was therefore better connected in longitude to the flare than was the Earth. Radio emission was seen at both spacecraft. However, by ∼60 kHz, the event at Wind was very delayed and the leading edge of the burst was essentially parallel to the plasma line. (The leading edge feature above ∼80 kHz is caused by receiver saturation). At Ulysses the burst drifted to lower frequencies but faded before reaching the plasma line, probably because the electron event was relatively weak. Nevertheless the burst leading edge, if extrapolated, would intercept the plasma line, unlike the situation at Wind. Electrons were seen at Ulysses several hours before such an extrapolation consistent with the relative timing between electrons and radio bursts in the previous events. At ACE the electron background was relatively high but there was no evidence of a new injection of electrons near Earth. There was an event in protons but it is was very delayed and not obvious in the time period illustrated. These protons were unlikely to be related to the type III burst because they arrived too late, and were probably accelerated at a CME-driven shock. Evidence of such a shock is the very weak, slowly drifting (type II-like) emission near 1000 kHz at 0400 UT. (Low-frequency shock emission is also seen in Figures 3a and 4a but it is faint in comparison with the illustrated type III bursts.)

[17] During the period in Figure 5b, there was ongoing storm activity seen at Ulysses and Wind extending to a few hundred kHz. Both spacecraft saw at least five radio bursts. Based upon coronagraph observations of a large CME and the absence of a flare, the most prominent burst was probably associated with an event behind the east limb of the Sun at about 2355 UT on May 29 2001. Ulysses was at 10°N off the west limb of the Sun at 1.3 AU. Assuming the active region was at about 95°E, Ulysses would have been connected to a location about 92° from the event, equivalent to an event behind the west limb as observed at Earth. The radio burst did not extend to the plasma line (∼20 kHz) at Wind but did so at Ulysses. There was an electron and proton event at Ulysses but not at Earth (note that the lack of IMP 8 data at Earth is not a data gap but a real lack of protons in the 24–29 MeV energy range). The important point to note is that the type III burst only extends down to the local plasma frequency at the spacecraft where energetic particles are also detected, again suggesting that the type III burst-producing electrons are a component of the particle population local to the spacecraft.

[18] The final multispacecraft events to be illustrated are ones in which a particle event was seen on both spacecraft but was delayed at one relative to the other. The first event (Figure 6a) was associated with a flare at ∼0100 UT on November 25, 2001 located at 07°N 50°E. The radio event, observed at both spacecraft, reached the plasma line earlier at Ulysses than at Wind. Unfortunately, there was a high particle background caused by two large particle events on the previous day. Ulysses observed a slowly increasing particle event but the start time is obscured because of the background. Ulysses was at its most southerly extent (−80°) and 2.3 AU, and with a connection angle of −26°. At Earth there was a very slowly rising particle event (consistent with the eastern flare location) only seen in the days following the interval illustrated. Again, the faster drifting burst toward the plasma line at Ulysses may be associated with a more rapid particle intensity increase at this spacecraft.

[19] The event of Figure 6b occurred late on August 15 2001. At the time, Ulysses was at 63°N and 34° west of Earth at 1.6 AU. The related CME clearly originated behind the west limb in the southern hemisphere. Radio emissions above 1 MHz were very faint at Wind, consistent with the

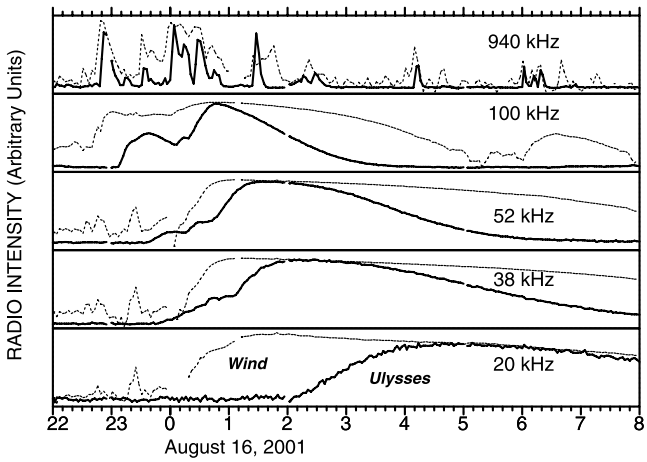

Figure 7. Intensity profiles at 5 similar frequencies at Wind and Ulysses during part of the interval shown in Figure 6b. Each profile is shown on a scale such that the burst extends almost to the full height of the panel. The profiles are quite similar at 940 kHz but become dissimilar at lower frequencies. At the lowest frequency shown there is a dramatic difference in the starting times of the emission; they differ by about 2 hours.

solar event location but were strong at lower frequencies, even at 20 kHz just above the plasma line. The radio event was also strong at Ulysses but faded before reaching the plasma line.

[20] This event of Figure 6b is a particularly good example in which individual frequency radio intensity profiles (i.e. cuts across the spectrum) through the event can be compared at each spacecraft. (In other events, AKR or other radio bursts often confuse the situation.) Figure 7 shows profiles at five frequencies chosen to be as close as possible at the two spacecraft and evenly distributed in 1/f space (equivalent to distance from the Sun). The vertical (logarithmic) scale in each panel is relative and chosen so that the heights of the profiles from each spacecraft (thicker lines = Ulysses; thinner, dashed curves = Wind) at that particular frequency are closely matched. The drift of the prominent emission associated with this event to lower frequencies as a function of time at both spacecraft is very evident. Furthermore, the drift is slower at Ulysses and the lowest frequency emission commences some two hours later than at Wind. The electron data shown in Figure 6b illustrate that the radio delay is matched by the delay in arrival time of electrons at the two spacecraft. Electrons and protons were seen at both spacecraft (Figure 6b). However, the onset was delayed and slower at Ulysses than at Earth. Again this appears to be consistent with the relative delays of the radio bursts seen for other events.

3. Discussion

3.1. Radio Emission Visibility

[21] The data presented above imply that type III radio emission observed by a spacecraft at frequencies near the local plasma frequency is generated when electrons arrive in the vicinity of the spacecraft. This might seem obvious, but it is not consistent with previous interpretations of type III bursts which suggest that, because of considerable radio scattering in the interplanetary medium, radiation is visible from sources in the heliosphere quite remote from the spacecraft. Indeed, the examples shown here of simultaneously observed events at Ulysses and Wind support the picture that type III emission at frequencies well above the plasma frequency is highly visible over wide regions of the heliosphere. The data in Figures 4 and 5 show, however, that the radio bursts are clearly seen on both spacecraft *only* in the frequency range 1MHz to above 50 kHz. At lower frequencies the visibility of the burst may be greatly reduced at one or other of the spacecraft. It has also long been recognized that the radial gradient of the refractive index near the plasma frequency will cause radiation, initially emitted in any transverse direction, to bend outward [cf. *Wild et al.*, 1954] making the source region invisible from points at the same radius but different longitudes or latitudes. Therefore radiation near the local plasma frequency must be caused by electron streams in the vicinity of the spacecraft and not by scattering from distant sources. Thus as the emission frequency approaches the local plasma frequency, the observations become more and more dominated by the part of the source closest to the observer. This explains why centroids of type III radio emission always track to the observer [*Reiner and Stone*, 1988]. It also implies that different spacecraft will observe different intensity-time profiles and arrival times at low frequencies. In contrast, at frequencies well above the local plasma frequency, all observers will receive emission from the complete electron source and so they will observe similar radio profiles (except above $\sim$1 MHz if the source is occulted). The directions to the centroid of the radio emission will also lie along an approximate spiral structure [e.g., *Reiner et al.*, 1995] for frequencies well above the local plasma frequency but at lower frequencies the positions will appear to bend toward the spacecraft.

[22] The observations are consistent with the suggestion that when the burst emissions approach the local plasma frequency, the electrons have reached the observation point and the radiation is produced near the spacecraft. This has been verified by simultaneous electron observations. Although these electron observations are at an energy higher than the electrons responsible for the radio emission ($\sim$40 keV versus $\sim$8 keV) there is little evidence to suggest that these electrons are of separate populations. For example, *Krucker et al.* [1999] find that, in the majority of the cases that they studied, the 1 AU arrival times of few keV and >25 keV electrons are consistent with their being accelerated at the same time. Furthermore, there are no significant spectral breaks in the electron spectra in the 1–100 keV energy range [e.g., *Lin et al.*, 1996]. This means that, when the emission extends close to the local plasma frequency, there is magnetic connection between the source of the (few keV and more energetic) electrons and the observer. Since protons appear to follow similar paths, this suggests that there is also magnetic connection for protons.

3.2. Radio Delays

[23] The fact that type III bursts do not drift at the same rate when viewed from different spacecraft was first systematically investigated by *Lecacheux et al.* [1989]. They found that the difference in burst arrival times at a fixed frequency increased with increasing separation between Voyager and

ISEE-3 with delays of up to 15 minutes at 233 kHz. They also found that the delays increased as inverse frequency so that at 23 kHz (which is close to a typical plasma frequency at 1 AU) one might expect a delay of more than 2 hours. In addition they found that the bursts with the largest delays tended to have the largest sizes and to show the largest decrease in intensity between the two spacecraft measurements. *Lecacheux et al.* [1989] discuss the possible reasons for the delays. They conclude that scattering and refraction of the radio emission is inadequate to account for the longest delays. For example, consider the delay of ~2 hours observed between Ulysses and Wind radio profiles at the same frequency shown in Figure 7. It is hard to understand how photons could remain in the vicinity of 1 AU for such long periods after emission; in a period of ~2 hours they will be refracted outwards and will travel ~15 AU.

[24] One possibility that *Lecacheux et al.* [1989] suggest for the delays is that the spacecraft with the delayed emission received only harmonic emission. It is known that fundamental emission is more focused. However this explanation is not tenable for the event of Figure 7. Assuming a density decreasing with distance from the Sun in the same manner at all longitudes then if the 20 kHz plasma level is at 1 AU (consistent with what is measured at Wind) then 20 kHz harmonic, which is produced at the 10 kHz level, will come from 2 AU. Thus for Ulysses to be detecting 20 kHz harmonic emission just after 0200 UT on August 16 the ~8 keV electrons that are responsible for the radio emission should be at 2 AU by this time. However we see in Figure 6b that even the 38–53 keV electrons have not arrived at Ulysses by this time.

[25] Another possibility discussed by *Lecacheux et al.* [1989] is the speed of the responsible electrons. They suggest a model in which the electrons are faster in the core of the stream than on the edges. However they found that a speed variation of more than 45% would be required to explain the longest delays and they thought that such a variation was unsupported by electron observations. Nevertheless Figures 3–6 show that the variations in electron arrival times are consistent with such a group speed variation. Note also that in a model developed to explain type III observations *Reiner and Stone* [1988, 1989] find that the observations can be modeled very well provided that they incorporate a longitudinal gradient in the electron arrival times at each plasma level i.e. that the electrons moving along the centroid of the electron beam arrive at the appropriate distance from the Sun first and that those at the edges of the beam arrive later. Such a model does explain the radio delays but how do we account for the observed particle delays?

3.3. Combining Radio and Particle Observations

[26] Delays in particle arrival at 1 AU are conventionally attributed to processes at the Sun since it is usually assumed that once in the solar wind, particles do not cross field lines and remain on the lines where they were first deposited. In particular, the particle delays are usually considered to represent the time it takes a shock to travel across the Sun and to deposit particles on an observer's field line. However we find that the radio delays, which extend up to several hours, are much longer than the durations of the radio bursts at the Sun (i.e., at high frequencies), typically 15–20 minutes for large events. Thus in the standard explanation, one would need to hypothesize that the "delayed" shock-accelerated electrons leave the Sun without generating radio emission. Highly beamed radiation not seen by a poorly connected observer can be ruled out on the basis of the high visibility of bursts between 1 MHz and about 50 kHz observed by different spacecraft.

[27] Suppose the delay were imposed at the Sun because the electrons undergo lateral transport in the corona after acceleration. Although it is possible that the delayed electrons might not initially produce radio emission it seems unlikely that the radiation would turn on in such a way to mimic a progressive delay in the interplanetary medium. Recall that *Lecacheux et al.* [1989] found that the radio delays were inversely proportional to frequency i.e., proportional to distance from the Sun. Also the continuity of the bursts from ~10 MHz to ~50 kHz appears to be inconsistent with such a hypothesis.

[28] The simplest interpretation of the radio data is that the electrons, and hence ions, cross the average interplanetary magnetic field direction much more easily than is currently believed. Significant cross-field transport has also been invoked by *McKibben et al.* [2001] to account for the uniformity in particle intensities seen for days after events observed at widely separated spacecraft. The nature of this transport process is not known but it is a topic of considerable interest because its existence is required to explain the solar modulation of cosmic rays and the escape of cosmic rays from the Galaxy. For recent discussions on the topic of perpendicular transport see *Giacalone* [1998] and *Jokipii* [2001].

[29] Figure 2 suggests that the acceleration region in the low corona that provides good magnetic connection (as evidenced by short radio delays) is quite extensive and may be as large as 100° in some events. (Such a region corresponds to the "open cone" of *Lin* [1970] and the "fast propagation region" of *Reinhard and Wibberenz* [1974]). In *Cane et al.* [2002] it was found that the type III bursts associated with high intensity, long lasting SEP events are associated with large CMEs and it was suggested that the responsible electrons were accelerated in the reconnecting/flaring regions caused by these CMEs. Such a region could be of the order of 100° in extent. For poorly connected events cross-field transport means that particles can be still be detected without the necessity of a shock to deposit particles on the observer's field line.

[30] Of course, CMEs do drive shocks that are observed in the interplanetary medium and are known to accelerate particles [*Cane et al.*, 1988]. However it is not clear what fraction of the population in large particle events is generated by these shocks. In particular, how are the particles accelerated at event onset when, perhaps, the CME shock is not yet formed or the acceleration process not yet efficient? *Cliver et al.* [1995] (see also *Cane* [1996]) have pointed out that another problem with CME-driven shocks producing early particles is that east limb source regions imply connection angles of about 150°, which is considerably larger than the half-sizes of the shocks which CMEs create in the interplanetary medium. As an alternative we suggest that particles reach the observer from poorly-connected source regions by some mechanism of cross-field transport. Finally we note that when the particle data are considered in isolation from the radio observations one can conclude as

did *Lin* [1970] that "we cannot rule out an interplanetary model ..but we feel that the profile of the electron events ..on solar longitude . . .indicates that the behaviour of the events is governed by processes occurring in the solar atmosphere". Likewise, many of the radio observations can be explained by invoking scattering of the radiation or a switch from fundamental to harmonic mode. However, in combination, it would seem that the most probable explanation is that particles cross the mean field in the interplanetary medium.

4. Summary

[31] We have used radio observations to demonstrate an intimate and systematic connection between flare acceleration in the low corona and electrons arriving at a spacecraft. Although not conclusively proven the observations of the same event from separate locations in the heliosphere are consistent with the following scenario: In large SEP events there is a significant population of particles accelerated in the flare process, both electrons and ions, which escape to the interplanetary medium. The low-energy electrons produce type III radio emission as they propagate outward along the interplanetary magnetic field, indicating the trajectory of the particles, including the higher energy electrons and of the ions. If an observer is magnetically connected to the source region, up to $\pm 40^\circ$ for more energetic events, particles arrive within minutes to about an hour (depending on their energy) and are accompanied by a type III burst that drifts rapidly to the observer's plasma frequency without a significant reduction in intensity. The lowest frequency emissions commence as the radio generating electrons start to arrive. If an observer is poorly connected to the source region a strong type III burst may be seen at high frequencies, corresponding to electrons at some distance from the Sun (within $\sim$0.5 AU for a 1 AU observer), but then because of refraction and beaming of the radiation away from the observer the emission becomes weaker at lower frequencies. The weak emission that is observed is generated by some electrons that leak away from the main stream through some form of cross-field transport. Eventually the leakage particles may reach the observer and in these cases radio emission near the local plasma frequency will be detected, again at the time when the low-energy electrons arrive. The cross-field leakage process may take up to four hours for a poorly connected observer near 1 AU. The radio data suggest that this process occurs in the interplanetary medium.

[32] **Acknowledgments.** The use of the data made available via the NSSDC CDAWeb is acknowledged. HVC thanks a number of colleagues for advice and encouragement including Bob MacDowall, Gerd Wibberenz, Paul Evenson, Ian Richardson, Ed Cliver, Tycho von Rosenvinge and Iver Cairns. This work was partially funded by a NASA contract with USRA and by the NSF under grants ATM-9819798 and ATM-0207221.

[33] The Editor thanks Sang Hoang and Mukul R. Kundu for their assistance in evaluating this paper.

References

Bastian, T. S., A. O. Benz, and D. E. Gary, Radio emission from solar flares, *Ann. Rev. Astron. Astrophys.*, *36*, 131, 1998.

Bougeret, J.-L., et al., WAVES: The radio and plasma wave investigation on the WIND spacecraft, *Space Sci. Rev.*, *71*, 231, 1995.

Cane, H. V., Longitudinal extents of coronal/interplanetary shocks, in *High Energy Solar Physics*, edited by R. Ramaty, N. Mandzhavidze, and X. M. Hua, pp. 124, AIP, Woodberry, N.Y., 1996.

Cane, H. V., D. V. Reames, and T. T. von Rosenvinge, The role of interplanetary shocks in the longitude distribution of solar energetic particle events, *J. Geophys. Res.*, *93*, 9555, 1988.

Cane, H. V., W. C. Erickson, and N. P. Prestage, Solar flares, type III radio bursts, coronal mass ejections and energetic particles, *J. Geophys. Res.*, *107*(A10), 1315, DOI 10.1029/2001JA000320, 2002.

Cliver, E. W., S. W. Kahler, D. F. Neidig, H. V. Cane, I. G. Richardson, M.-B. Kallenrode, and G. Wibberenz, Extreme "propagation" of solar energetic particles, *Proc. 24th Inter. Cosmic Ray Conf.*, *4*, 257, 1995.

Dulk, G. A., Type III solar radio bursts at long wavelengths, in *Radio Astronomy at Long Wavelengths*, *Geophys. Monogr. Ser.*, vol. 119, edited by R. G. Stone et al., p. 115, AGU, Washington, D.C., 2000.

Dulk, G. A., Y. Leblanc, P. Robinson, J.-L. Bougeret, and R. P. Lin, Electron beams and radio waves of solar type III bursts, *J. Geophys. Res.*, *103*, 17,233, 1998.

Giacalone, J., Cosmic-ray transport coefficients, *Space Sci. Rev.*, *83*, 351, 1998.

Jokipii, J. R., Latitudinal heliospheric magnetic field: Stochastic and causal components, *J. Geophys. Res.*, *106*, 15,841, 2001.

Krucker, S., D. E. Larson, R. P. Lin, and B.J. Thompson, On the origin of impulsive electron events observed at 1 AU, *Astrophys. J.*, *519*, 864, 1999.

Lanzerotti, L. J., et al., Heliospheric instrument for spectra, composition and anisotropy at low energies, *Astron. Astrophys. Suppl.*, *92*, 349, 1992.

Leblanc, Y., G. A. Dulk, and S. Hoang, The low radio frequency limit of solar type III bursts: Ulysses observations in and out of the ecliptic, *Geophys. Res. Lett.*, *22*, 3429, 1995.

Lecacheux, A., J.-L. Steinberg, S. Hoang, and G. A. Dulk, Characteristics of type III bursts in the solar wind from simultaneous observations on board ISEE-3 and Voyager, *Astron. Astrophys.*, *217*, 237, 1989.

Lin, R. P., The emission and propagation of $\sim$40 keV solar flare electrons II The electron emission structure of large active regions, *Sol. Phys.*, *15*, 453, 1970.

Lin, R. P., Energetic solar electrons in the interplanetary medium, *Sol. Phys.*, *100*, 537, 1985.

Lin, R. P., et al., Observation of an impulsive solar electron event extending down to $\sim$0.5 keV energy, *Geophys. Res. Lett.*, *23*, 1211, 1996.

Meyer-Vernet, N., and C. Peche, Tool kit for antennae and thermal noise near the plasma frequency, *J. Geophys. Res.*, *94*, 2405, 1989.

McGuire, R. E., T. T. von Rosenvinge, and F. B. McDonald, The composition of solar energetic particles, *Astrophys. J.*, *301*, 938, 1986.

McKibben, R. B., et al., ULYSSES COSPIN observations of the energy and charge dependence of the propagation of solar energetic particles to the Sun's south polar regions, *Proc. 27th Inter. Cosmic Ray Conf.*, *8*, 3281, 2001.

Reiner, M. J., and R. G. Stone, Model interpretation of type III radio burst characteristics I. Spatial aspects, *Astron. Astrophys.*, *206*, 316, 1988.

Reiner, M. J., and R. G. Stone, Model interpretation of type III radio burst characteristics: II. Temporal aspects, *Astron. Astrophys.*, *217*, 251, 1989.

Reiner, M. J., J. Fainberg, and R. G. Stone, Large scale interplanetary magnetic field configuration revealed by solar radio bursts, *Science*, *270*, 461, 1995.

Reinhard, R., and G. Wibberenz, Propagation of flare protons in the solar atmosphere, *Sol. Phys.*, *36*, 473, 1974.

Simnett, G. M., Energetic particle characteristics in the high-latitude heliosphere near solar maximum, *Space Sci. Rev.*, *97*, 231, 2001.

Simpson, J. A., et al., The Ulysses cosmic ray and solar particle investigation, *Astron. Astrophys. Suppl.*, *92*, 365, 1992.

Stone, R. G., et al., The unified radio and plasma wave investigation, *Astron. Astrophys. Suppl.*, *92*, 291, 1992.

Wild, J. P., J. D. Murray, and W. C. Rowe, Harmonics in the spectra of solar radio disturbances, *Aust. J. Phys.*, *7*, 439, 1954.

H. V. Cane, Code 661, Laboratory for High Energy Astrophysics, NASA Goddard Space Flight Center, Greenbelt, MD 20771, USA. (hilary.cane@utas.edu.au)

W. C. Erickson, Bruny Island Radio Spectrometer, Lighthouse Road, Bruny Island, Tasmania, 7150 Australia. (bill.erickson@utas.edu.au)